Tutores

Dra. Maria Sarret i Pons
Departament de Ciència de Materials i Química Física.

Dra. Elisabet Playà i Pous
Facultat de Ciències de la Terra. Departament de Mineralogia, Petrologia i Geologia aplicada.

Grau de Química

Treball Final de Grau

Green Rust: a review on its crystallographic structure, redox flexibility and role in reducing soil pollutants.

Green Rust: una revisió sobre la seva estructura cristal·logràfica, flexibilitat redox i paper en la reducció de contaminants del sòl.

Enric Juanmartí i Guiluz

Gener 2021

Universitat de Barcelona

B:KC Barcelona Knowledge Campus
Campus d'Excel·lència Internacional

Vull agrair tota l'ajuda que he rebut de les meves tutores, la Maria Sarret i l'Elisabet Playà a l'hora de fer aquest projecte. També a la Diana Puigserver, per haver-nos deixat participar del seu projecte de descontaminació d'etens clorats d'un aqüífer. Agraeixo l'esforç que heu fet tot i les difícils condicions en les que ens ha tocat fer aquest treball.

REPORT

CONTENTS

1. SUMMARY

Green Rusts (GRs) are mixed hydroxysalts of Fe(II) and Fe(III) that belong to the Layered Double Hydroxide (LDH) group. Their crystallographic structure can be summarised as a stacking sequence of $Fe(OH)_2$ layers with some Fe(III) cations substituting that provides a positive charge, and interlayers composed of anions and water molecules. Different types of GRs, depending on the anions in the interlayer, have been described and synthetised, and a mineral counterpart, fougerite, is found in hydromorphic soils. One of the most important features of GRs is their redox flexibility. On one hand, it implies that are very unstable compounds that easily oxidise, so special procedures must be followed to avoid it when working with natural or synthetic samples. On the other hand, its redox flexibility provides them an important role in reducing pollutants in hydromorphic soils, particularly the chlorinated ethenes.

Keywords: Iron, Hydroxide, Green Rust, Fougerite, Hydromorphic soil, Chlorated ethenes.

2. RESUM

Els anomenats *Green Rusts* són hidroxisals mixtes de Fe(II) i Fe(III) que pertanyen al grup dels Hidròxids Doble Laminars (LDH). La seva estructura cristal·lina es pot descriure breument com una seqüència de capes de $Fe(OH)_2$ que tenen alguns cations Fe(III) com a substituts, la qual cosa els proporciona una càrrega positiva, i *interlayers* compostes de molècules d'aigua i anions. Segons l'anió que tenen a la *interlayer*, s'han sintetitzat i descrit diferents tipus de GRs, i l'homòleg mineral, anomenat fougerita, s'ha detectat en sòls hidromòrfics. Una de les característiques principals d'aquests compostos és la seva flexibilitat redox. Per una banda, això implica que són compostos molt inestables, que ràpidament s'oxiden i, per tant, s'han de seguir uns protocols específics quan es treballa amb mostres, bé siguin naturals o sintètiques, per evitar aquesta oxidació. Per altra banda, aquest comportament redox li atorga un paper important a l'hora de reduir contaminants del sòl, particularment els etens clorats.

Paraules clau: Ferro, Hidròxids, Green Rust, Fougerita, Sòl hidromòrfic, Etens clorats.

3. INTRODUCTION

3.1. GREEN RUST: THE FE(II-III) HYDROXYSALTS.

Iron is one of the most abundant elements on Earth, and it is mostly found on Earth's core. In the Earth's crust conditions, iron is found as one of its oxidated forms. One of these oxidated forms of iron are the mixed hydroxysalts of Fe(II) and Fe(III) called Green Rusts (GR) [1]. Their crystallographic structure is defined since they belong to the Layered Double Hydroxide (LDH) group, and its generic chemical composition is defined by $[Fe(II)_{(1-x)} \cdot Fe(III)_x \cdot (OH)_2]^{x+} \cdot [(x/n) \cdot A^{n-} mH_2O]^{x-}$ [2], where x is the ratio [Fe(III)/Fe_{total}], and A^{n-} is an anion, typically OH^-, Cl^-, CO_3^{2-} or SO_4^2, although other GRs have been described [3]. Depending on the anion in the interlayer two groups of GR are described, GR1 and GR2: GR1 are those with planar anions, and GR2 those with tetrahedral anions.

GRs are unstable compounds that rapidly oxidise to more oxidated iron oxides such as magnetite or Fe(III) oxyhydroxides [4]. This redox behaviour will have consequences in the samples treatment as well as in the techniques used to determine its crystallographic structure.

In natural conditions, GRs can be found in hydromorphic soils, i.e., those soils saturated temporary or permanent with water and where the sources of oxygen are restricted, which leads to anaerobic conditions over long periods of time [5], [6]. In these hydromorphic soils, it is typical to observe green-bluish colours that turn into ochre when they are in contact with the outer atmosphere.

3.2. PRECEDENTS

The green-bluish colour observed in hydromorphic soils was historically attributed to the presence of mixed-valence Fe(II)-Fe(III) compounds [7], without specifying their exact composition or formula. Later, GRs were synthetised and named by Bernal et al. [1]. GR has also been identified as a product of steel corrosion, for example in marine water [8]. Evidence of natural formed GR were found and confirmed first in a sludge in Thorsbro (Copenhagen, Denmark) [9] and then in an hydromorphic soil in Fougères (Brittany, France) [10]. The exhaustive study of the

samples from Fougères led to the approval of the International Mineralogical Association (IMA) as a new mineral, with the number 2003-057 and it was officially called fougerite. Since then, both synthetic and natural GRs have been characterised, and their properties have been studied.

3.3. WORK MOTIVATION

Is known that iron oxides (including GRs) have an important role in natural soils, acting as an electron donor, which means that have an important reductor power [11], [12]. In particular, GRs are found to show an unusual redox flexibility, so they are able to reduce many pollutants in soils, such as NO_3^- [13], Cr(VI) [14] or chlorinated ethenes [15]. The necessity of a review work about GR and its possibilities to reduce pollutants arose to establish the theoretical basis that helps to understand the role of GR in a remediation process of an aquifer polluted by chlorinated ethenes.

4. OBJECTIVES

The objective of this work is to do a review on published bibliography about GR and to understand its main characteristics, focusing in:

- Study how the characterisation of the natural mineral and the synthetic counterparts is done, which techniques are used to analyse them, and which protocols are followed.

- Describe crystallographic structure for GR, both natural and synthetic.

- Summarise the knowledge about the thermodynamics of GRs and its redox flexibility.

- Introduce the role that can have these compounds, among other Fe(II) containing compounds, in the remediation of aquifers polluted by chlorinated ethenes.

5. METHODS

To search the bibliography consulted, the databases that were used are SciFinder and GeoRef. In order to have a general view of the subject, publications between the late 90s and 2015 were reviewed.

Searches were done using “Green Rust” as a keyword and adding the necessary other keywords for each one of the topics of interest, such as “Crystallographic structure”, “Mössbauer” or “Dechlorination”. Then, all the results were organised and structured according to the sections addressed.

6. RESULTS AND DISCUSSION

6.1. CHARACTERIZATION

The study of the GRs crystallographic structure is not an easy task, because they are unstable compounds that are formed from $Fe(OH)_2$ and that rapidly oxidises to final corrosion products like Fe(III) oxyhydroxides and magnetite. Nevertheless, it has been widely studied the structure for both synthetic GR and natural Fougerite.

6.1.1. Sample conservation and treatment

Since GRs are easily oxidable compounds, special care must be taken when samples are collected or synthetised to avoid oxidation to more stable phases (such as goethite, lepidocrocite or Fe(III) oxyhydroxides like schwertmannite) in contact with air. The colour of the sample is a good indicator of the oxidation state of it, while a green-bluish colour indicates the presence of GR, colours grey or ochre indicates more oxidated forms. It is observed that in 10 minutes, the original green-bluish colour of the samples containing GR can be already lost [16].

For the synthetic GRs, Hansen [17] described the procedure to synthetise carbonate GR, introducing a nitrogen flow through the solution where synthesis is carried on, during the reaction and afterwards. The GR crystals are wetted with glycerol or glucose-saturated water once obtained, and these treatments are shown to avoid oxidation and to stabilise GR structure. Even

though, in most posterior studies, only a procedure of sheltering the flask that contains the samples and maintaining them under anoxic N_2 atmospheres is described [18], [19]. If analyses of dissolved species are pretended to be done, they have to be carried out in an acid medium, because in a basic medium Fe(II) can oxidise and form Fe(III) oxyhydroxides [20].

For natural solid samples, they must be protected from air during the extraction and treatments in laboratory. To ensure it, samples are kept in anoxic chambers. In addition, samples are taken in large volumes and small aliquots are extracted from the core to analyse them. A good criterion to know if samples are being correctly preserved is the permanence of the blue-green original colour, as explained previously, a change of colour to ochre means that the sample has been oxidated [10], [21].

Natural water samples must be treated with similar procedures, ensuring no contact with air or light [22]. If non-conservative parameters (such as Temperature, pH, redox potential, Fe(II) conc. or NO_2^- conc.) of the water samples are necessary to be measured, it must be done in situ [5].

Although general procedures for samples treatment and conservation are described [17], many studies seem to assume them and they do not elaborate on which exactly treatments and procedures are they working with [4], [8], [23].

6.1.2. Main techniques used to define the crystallographic structure

The main techniques used to study the crystallographic structure of the GRs are Transmission Mössbauer Spectroscopy (TMS) and X-Ray Diffraction (XRD) [21], [24], therefore will be analysed for every GR case studied.

6.1.2.1. Transmission Mössbauer Spectrometry (TMS)

TMS is usually performed in order to understand how cations and anions are distributed along the layers and interlayers. This technique uses the absorption of gamma ray by a solid to analyse the nuclei and their environment. Two types of nuclear interactions are studied for the GRs case (Fig. 1):

- Isomer shift (δ): describes a shift in the resonance energy of the nucleus due to differences in nearby electron densities. That hyperfine parameter helps to assign the

oxidation state of the atom, concretely in Fe case, Fe(II) cations have higher isomer shifts and Fe(III) cations lower.

- Quadrupole splitting (Δ): describes the effect that the surrounding electric field gradient has on the energy levels of the nucleus. That hyperfine parameter helps to assign the oxidation state of the atom and the spin state.

Thus, TMS allows us to assign each one of the spectra peaks to a specific kind of Fe cation depending on the atoms they are surrounded by since it is sensitive only to ^{57}Fe nuclei.

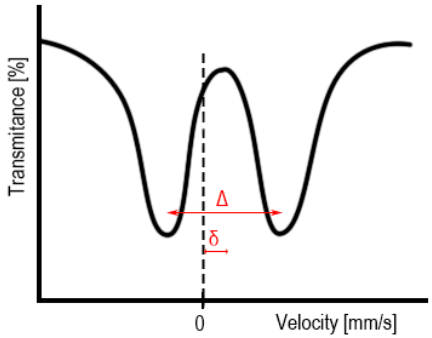

Figure 1. TMS spectra and its hyperfine parameters δ and Δ.

If GR samples are pretended to be analyzed with TMS, special care must be taken to avoid unwanted oxidation. A procedure consisting in keeping the samples frozen under dry ice before the analysis and taking the spectra under He atmosphere and in a bath cryostat (at 120 K) is described [25], [26]. Posterior studies registered spectra at 78 K, preparing the sample under inert atmosphere and also using a cryostat [27].

6.1.2.2. X-Ray Diffraction (XRD)

XRD analyses provide valuable information about the reduced coordinates of atoms and interatomic distances, and it is also an analytic tool to distinguish between GR1 and GR2. GR1 compounds have a characteristic peak d_{003} between 7.5 Å and 8.0 Å, while GR2 compounds have a characteristic peak d_{001} between 11.0 Å and 11.6 Å [21].

This technique is based on the interaction between the X-Rays and a crystalline structure. The X-Rays are scattered in every direction, those that obey the Bragg's Law create a constructive interference and its directions are used to deduce the crystallographic structure.

For XRD analyses, GR samples must be rinsed with glycerol (a 1:1 solution of glycerol to deoxygenated ultrapure water) in an anoxic chamber, so they can be in contact with air and maintain its structure [28].

6.1.3. Other techniques used

Even though the techniques that give us more information are the TMS and the XRD, other techniques have been performed to obtain valuable information about the GRs structure.

6.1.3.1. Transmission Electron Microscopy (TEM) and Scanning Electron Microscopy (SEM)

Analyses with TEM and SEM have allowed to observe the GR crystals, that have a well-defined plane and hexagonal shape. It means that crystals have an anisotropic growth, the growth of the lateral faces is faster than the growth of the main face. Crystals with a diameter within the range 10-1000 nm have been reported, depending on the synthesis method (for synthetic GRs) or the sample treatment (for fougerite). Nevertheless, the most frequent ones have an approximate diameter of 500 nm. Different crystal thicknesses have also been reported. Actually, it has been demonstrated that a positive correlation between the thickness and diameter of the crystals does exist [28]–[33]. Electron diffraction patterns (spots that correspond to a satisfied diffraction condition) have also been obtained with TEM. [29], [34].

TEM and SEM are based on the study of the electrons that are projected towards the solid sample. In TEM the electrons studied are those that go through the sample (primary electrons), while in SEM electrons emitted due to the excitation that produces the primary electrons, called secondary electrons.

Sample preparation for TEM and SEM analyses consists of diluting the solid sample into ultrapure water or ethanol and place a drop in the copper or gold grid. All procedure must be done under anoxic conditions [28], [29], [31].

6.1.2.2. Raman spectrometry

Raman spectrometry has been performed in both synthetic and natural GRs, and both showed characteristic bands at 427 and 518 cm^{-1}. This technique allows us to confirm the compounds identification, but it is not useful to distinguish between types of GRs. [21], [16]. This technique is based on analysing the few scattered photons by the surface of the solid that have a different frequency than the incident radiation (inelastic scattering).

6.1.2.3. Differential Scanning Calorimetry (DSC)

This technique, that measures the difference of heat that is needed to warm up a sample depending on its temperature, is used to obtain data about the water content in GR compounds, so it is possible to know the number of water molecules in the molecular formula [20].

6.1.4. Crystallographic structure of synthetic GRs

GRs belong to the layered double hydroxy (LDH) group. From a general point of view, the structure of the GR compounds can be described as a succession of $Fe(OH)_2$ positively charged layers, due to the presence of intercalated Fe(III) cations, alternated with periodic interlayers that contain anions and water molecules. An intuitive way to understand them is considering a basic $Fe(OH)_2$ structure where anions are intercalated and the global charge is balanced by substituting some Fe(II) cations with Fe(III) cations [24].

In order to discuss about the GR's structure, it's basic to differentiate between GR1 and GR2, a classification that was established by Bernal et al. [1] looking at the two types of XRD patterns that generates the two types of GR. GR1 group includes GR1(Cl^-), GR1(CO_3^{2-}), GR1(OH^-), GR1(SO_3^{2-}), GR1($C_2O_4^{2-}$) and GR1($HCOO^-$), that is, GR formed by planar anions [3], while GR2 group is formed by GR2(SO_4^{2-}) and GR2(SeO_4^{2-}), three-dimensional anions [20].

The three most studied GRs are GR1(Cl^-), GR1(CO_3^{2-}) and GR2(SO_4^{2-}) since they are representative of all the other cases. Therefore, the structure of these three cases will be analysed.

6.1.4.1. Crystallographic structure of GR1(Cl-)

GR1(Cl-) crystal structure it's assumed to be like the one of the mineral pyroaurite, which implies a Rhombohedral $R\bar{3}m$ space group with parameters a = 0.3190(1) nm and c = 2.385(6) nm [24].

As is represented in Figure 1a, the stacking sequence for a GR1(Cl-) is A, c, B, i, B, a, C, j, C, b, A, k… where A, B and C are OH^- layers, a, b and c are Fe cation layers and i, j and k, Cl^- interlayers. Easier to appreciate in Figure 1b, the OH^- anions in the layers generates octahedral holes, where Fe(II) and Fe(III) are positioned. The position of the Fe(III) cations is correlated with the position of the Cl^- in the interlayer, since a Cl^- shares its negative charge with one Fe(III) from the layer over and one from the layer below, as is widely described by Génin et al. [24]. Cl^- anions are placed in the interlayer randomly but they cannot be one immediately beside another one, leading to a maximum occupancy of (1/3) of the hexagonal path. The sites that are excluded for the Cl^- anions can be, also randomly, occupied by water molecules. At that point, it is important to understand that only one type of chemical environment exists for the Fe(III) cations, but it is necessary to distinguish between two types of Fe(II) cations, the ones that are under the influence of 2 Cl^- anions and the ones that have only water molecules as a neighbour and do not feel any anion influence. These two types of Fe(II) will be named as Fe(Cl^-) and Fe(H_2O) respectively.

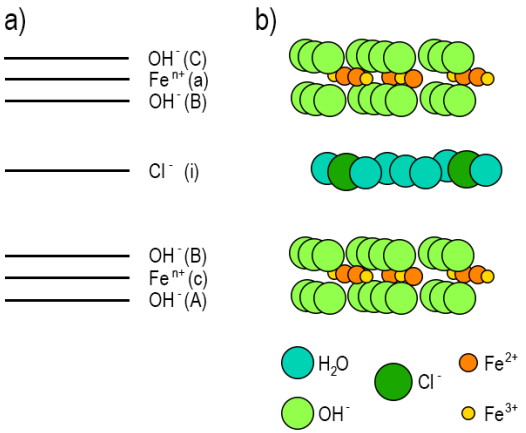

Figure 1. (a) Stacking sequence for GR1(Cl-). (b) Schematic representation of GR1(Cl-) structure [2], [24].

XRD has been performed in synthetic GR1(Cl^-) samples by Génin et al. [21], [35]. The reduced coordinates of atoms and interatomic distances obtained are summarised in Tables 1 and 2.

	x	*y*	*z*
Fe	0	0	0
O (OH^-)	0	0	0.375
O (H_2O)	0.1	0.1	0.5
Cl	0.25	0.25	0.5

Table 1. Reduced coordinates of atoms in GR1(Cl^-) [21].

Layer-layer distances [nm]		
Fe - OH^-: 0.099	OH^- - OH^- (hydroxide layer): 0.199	OH^- - interlayer: 0.298
Interatomic distances [nm]		
Fe - OH^-: 0.209	OH^- - OH^- (6x): 0.319	OH^- - OH^- (3x): 0.277
OH^- - H_2O: 0.300	OH^- - Cl^-: 0.309	Cl^- - H_2O (min): 0.320

Table 2. Interatomic distances in GR1(Cl^-) [21].

TMS analyses are performed, and in the Mössbauer spectres obtained for GR1(Cl^-) are basically fitted with three doublets (D_1, D_2 and D_3). D_1 and D_2 are attributed to the two types of Fe(II) cations in GR1(Cl^-), $Fe^{II}(H_2O)$ and $Fe^{II}(Cl^-)$ respectively, while D_3 is attributed to Fe(III) cations. This point is deeply discussed by Génin et. al. [24]. The data obtained from the TMS is compiled in Table 3.

Besides, from that TMS data it is possible and especially interesting to study the composition of GR1(Cl^-) since the relative area under the peaks gives us information about the proportion of every type of Fe^{n+} cation in the compound. The [Fe(III)]/[Fe_{total}] ratio is defined as *x* and it is directly proportional to the relation between the area under D_3 peak over the area under all the peaks. According to the relative abundances (RA) in Mössbauer spectra, the abundance of $Fe^{II}(Cl^-)$ must be the same as the abundance of Fe(III) (*x*), thus the abundance of $Fe^{II}(H_2O)$ must be (*1 - 2x*).

As it has said before, occupancy of Cl^- in the interlayer is as maximum (1/3), which implies a maximum x = 0.33, but experimentally GR1(Cl^-) with x = 0.25 have been obtained. The two samples shown in Table 3 show the two extremes of the composition domain, for x = 0.25 (when a ratio of RA 2:1:1 is shown) and for x = 0.33 (when the ratio is not 2:1:1 anymore). To sum up, GR1(Cl^-) can have a variable composition inside the domain $0.25 \leq x \leq 0.33$.

GR1(Cl^-) x = 0.25

T [K]	78		
	δ [mm s^{-1}]	***Δ***	***RA [%]***
D_1	1.26	2.88	48
D_2	1.25	2.60	24
D_3	0.47	0.41	24
W	1.37	3.36	4

GR1(Cl^-) x = 0.33

T [K]	20		
	δ [mm s^{-1}]	***Δ***	***RA [%]***
D_1	1.31	2.89	37
D_2	1.29	2.57	32
D_3	0.40	0.40	31
W			

Table 3. Hyperfine parameters obtained from TMS for different GR1(Cl^-) compositions. Depending on the experiment, the measurement temperature was different, and it is documented in the table [24], [18].

X-ray diffraction pattern and Mössbauer spectra for GR1(Cl^-), from where these data have been extracted, are shown in Appendix 1.

6.1.4.2. Crystallographic structure of GR1(CO_3^{2-})

Similar as GR1(Cl^-), since they are both GR1, GR1(CO_3^{2-}) has also an $R\bar{3}m$ space group with lattice parameters a = 0.3160(5) nm and c = 2.245(5) nm [24], and an equivalent stacking sequence. Unlike the Cl^- ions in GR1(Cl^-), every CO_3^{2-} ion needs 3 places in the hexagonal path, which means 2 negative charges for every 3 sites. For the stoichiometric GR1(CO_3^{2-}) i.e., when the value of the x = [Fe(III)]/[Fe_{total}] = 1/3, half of the places are occupied by CO_3^{2-} ion [19]. Apart from stoichiometric GR1(CO_3^{2-}), a wide range of x ratio values has been described, which will be the object of analysis in Section 6.2.2.

XRD has been performed for GR1(CO_3^{2-}) and atomic coordinates and interatomic distances are summarised in Tables 4 and 5.

	x	*y*	*z*
Fe	0	0	0
OH	0	0	0.37804
O	0.119(1)	0.881(1)	0.5(-)
C	0	0	0.167(2)

Table 4. Reduced coordinates of atoms in GR1(CO_3^{2-}) [36].

Interatomic distances [nm]		
Fe - OH^- (6x): 0.20957(14)	OH^- - C: 0.3331(48)	O - O: 0.2629(5)
OH^- - OH^-: 0.2736(3)	O - O: 0.2787(5)	C - O (3x): 0.1179(3)

Table 5. Interatomic distances in GR1(CO_3^{2-}) [36].

TMS has been performed to understand better the composition of GR1(CO_3^{2-}). First of all, it's important to note that the peaks assignation is the same as in the GR1(Cl^-) case analysed before: D_1 for $Fe^{II}(H_2O)$, D_2 for $Fe^{II}(CO_3^{2-})$ and D_3 for Fe(III). As is shown in Table 6, for an x = 0.33 ratio, there is one type of Fe(III) cation with an abundance of (1/3), and two types of Fe(II) cations, equivalent to the GR1(Cl^-) case, $Fe^{II}(H_2O)$ and $Fe^{II}(CO_3^{2-})$ with abundances of (1/2) and (1/6) respectively [24].

$GR1(CO_3^{2-})$ x = 0.33			
T [K]	20		
	δ [mm s^{-1}]	***Δ***	***RA [%]***
D_1	1.28	2.97	48±2
D_2	1.28	2.55	18±2
D_3	0.47	0.43	34±1
W			

Table 6. Hyperfine parameters obtained from TMS for different GR1(CO_3^{3-}) compositions [3].

6.1.4.3. Crystallographic structure of GR1(SO_4^{2-})

GR2(SO_4^{2-}) is the most typical and studied compound from the GR2 group. Some differences exist between these compounds and the ones described before, belonging at the GR1 group. GR2(SO_4^{2-}) has a trigonal structure ($P\bar{3}m1$ space group) with cell parameters a = 0.5524(1) nm, c = 1.1011(3) nm [20].

In Figure 2 it is possible to notice the main difference between GR1 and GR2 compounds: what the interlayer is composed of. While in GR1 one single plane of A^{n-} anions and water molecules composes every interlayer, in GR2 compounds there are two planes in each interlayer. Furthermore, the stacking sequence for these compounds is A, c, B, i, j… where A and B are OH^- layers, c are Fe cation layers and i and j the two anion and water molecules planes composing the interlayers. As a consequence of this interlayers composition, sulphate anions have always the sulphur atom and three of the oxygen atoms at the same plane as the water molecules, but the fourth oxygen atom is pointing towards the nearest cation layer (some of them point up and some of them point down), as can be observed in Figure 2. Actually, oxygen atoms are pointing to a specific cation site, which leads to think that a Fe(III) cation will be occupying that site, thus only one type of Fe(II) cation exists, it will be called $Fe^{II}(H_2O)$ since they are far from sulphate ions.

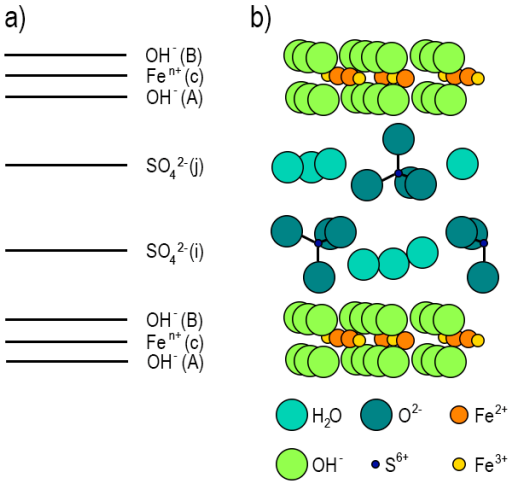

Figure 2. (a) Stacking sequence for GR2(SO_4^{2-}). (b) Schematic representation of GR1(SO_4^{2-}) structure [20].

XRD has been performed for GR2(SO_4^{2-}) synthesised samples, and atomic coordinates and interatomic distances are summarised in Tables 7 and 8.

	x	*y*	*z*
Fe(II)	2/3	1/3	0
Fe(III)	0	0	0
OH⁻	0.3250	0	0.0728(9)
H_2O	-0.234(6)	0.619(3)	0.663(3)
S(VI)	0	0	0.641(5)
O^{2-}_A	0	0	0.778(5)
O^{2-}_B	0.256	0	0.596(5)

Table 7. Reduced coordinates of atoms in GR2(SO_4^{2-}). O_A are the oxygen atoms placed at the same plane as the water molecules and O_B are those pointing at the Fe(III) cations [20].

Interatomic distances [nm]		
Fe(II) - OH^- (6x): 0.2030(4)	OH^- - OH^-(2x): 0.3110(4)	H_2O - OH^-: 0.3131(4)
Fe(III) – OH^- (6x): 0.1966(4)	OH^- - O_A: 0.243(4)	S - O_A: 0.1500
Fe(III) - O_A: 0.245(5)	H_2O - O_A: 0.297(7)	S - O_B (3x): 0.1500
OH^- - OH^- (2x): 0.2407(9)	H_2O - H_2O: 0.298(4)5	
OH^- - OH^-: 0.2512(9)	H_2O - O_B: 0.3068(4)	

Table 8. Interatomic distances in GR2(SO_4^{2-}) [20].

Finally, some information can be deduced from TMS data (shown in Table 9). Only two doublets appear in GR2(SO_4^{2-}) spectra, D_1 and D_3. As discussed previously, D_1 belongs to the unique Fe(II) cation that there exist on GR2(SO_4^{2-}), and D_3 to the Fe(III) cations. A ratio of abundances of 1:3 is observed, which means a x = [Fe(III)]/[Fe_{total}] = 0.33 ratio.

At this point, it is important to notice that three doublets (D_1, D_2 and D_3) are observed for GR1 compounds, while only two doublets (D_1 and D_3) are observed for GR2 compounds. Actually, this information is used for differentiating between the two types of compounds.

GR1(SO_4^{2-}) x = 0.33

T [K]	78		
	δ [mm s^{-1}]	***Δ***	***RA [%]***
D_1	1.27	2.88	66
D_2			
D_3	0.47	0.44	34
W			

Table 9. Hyperfine parameters obtained from TMS for different GR2(SO_4^{2-}) [24].

6.1.5. Crystallographic structure of Fougerite: the natural GR

GR was identified as a mineral for the first time in a gleisoil in Fougères (Brittany, France) in 1997, and identified as a GR by TMS and Raman spectroscopy [16]. Since then, this emplacement has been under study to determinate the nature of fougerite. These analyses have several difficulties to be carried out mostly because fougerite oxidises rapidly in contact with air, the total content of Fe in these soils is only about 3%, it is present in very small particles (around 500 nm), and it is not possible to separate fougerite from other minerals. To avoid these difficulties, only ^{57}Fe sensitive techniques must be used, i.e. ^{57}Fe TMS and X-ray absorption spectroscopy at the Fe *K* edge (XAS) [27].

Fougerite is assumed to have a GR like structure, since TMS [4], [27] and Raman [16] spectra are almost the same as for those synthetic ones, but the following topics must be considered.

6.1.5.1. Partial substitution of Fe(II) by Mg(II)

The main proof that this substitution occurs in natural GR is the presence of a D_4 doublet in the TMS spectra of fougerite that does not appear in any synthetic GR. The presence of this D_4 doublet clearly indicates a new type of Fe(III) cation caused by the neighbours Mg(II) cations. The exact quantity of Mg in a fougerite sample cannot be determined quantitatively, even though the RA of the D_4 doublet is directly proportional to the amount of Mg incorporated [5], [27].

A TMS spectrum of a natural fougerite sample is shown in Figure 3, where the four doublets are fitted.

The partial substitution of Fe(II) by Mg(II) leads to the following general formula for the GR mineral: $[Fe(II)_{(1-x)}Mg(II)_yFe(III)_x(OH)_{(2+2y)}]^{x+}[x/n\ A^{n-}\cdot m\ H_2O]^{x-}$ [27]. The presence of Mg cations stabilizes the mineral [21].

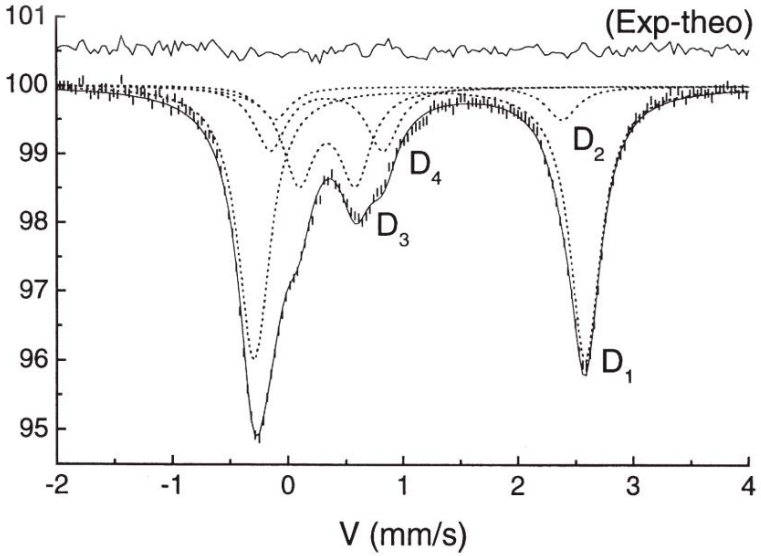

Figure 3. Mössabuer spectrum of a fougerite sample fitted with four doublets. [27]

6.1.5.2. Anion in the interlayer

Since with XAS and TMS we are not able to obtain enough information about which anion is in the interlayer, it has been the main unresolved question about the mineral. In the case of XAS, the spectra do not depend on the interlayer composition, and in the case of TMS, the RA do depend on the GR type, but it is not enough to assign one anion to the fougerite interlayers [27], [37].

The two most accepted theories about the anion in the interlayer are the following ones:

- Fougerite is a GR1(OH^-), described as a ternary solid solution of $Fe(OH)_2$, $Fe(OH)_3$ and $Mg(OH)_2$, but a synthetic counterpart has not been synthetised at the laboratory [16], [37], [38].
- Fougerite is GR1(CO_3^{2-}), that continuously oxidises into GR(CO_3^{2-})*, an oxidated form named oxyhydroxycarbonate GR, following a deprotonation reaction that will be discussed in section 6.2.2. [4], [19], [24], [39].

Anyway, the most realistic proposal is that depending on the conditions of the soil, different anions could be in the interlayer, including OH^-, CO_3^{2-} and even Cl^-, thus we can speak about OH-fougerite, carbonate-fougerite or chloro-fougerite [40].

6.1.5.3. Variable x ratio

The ratio $x = [Fe(III)]/[Fe_{total}]$ is found to be between 0.33 and 0.67 in fougerite. Studies done with natural samples from Fougères (Brittany, France) demonstrate that the value of the ratio *x* depends on, at least, these four variables:

- The depth. A progression from minimum *x* values to maximum *x* values is observed. In deeper soils, more reductomorphic, more ferrous fougerite (i.e. lower *x* values) is found, while ferric fougerite (i.e. higher *x* values) is more common in oximorphic upper soils [5], [37], [41].
- The level of the water table. The fluctuations on that level leads to rapid variations of the aerobic or anaerobic conditions, which involve variations on the *x* ratio value [41].
- The season. Since it also influences the water present in the soil. The cycle that occurs over the year is fully described by F. Feder et al. in [41]. In more rainy seasons, fougerite becomes more ferric as water brings O_2 at the soil [19].
- The amount of Mg^{2+}. The ratio *x* rises as more Mg is introduced in the structure [21].

6.2. THERMODYNAMIC ANALYSIS AND REDOX FLEXIBILITY

Is known that Fe is a key element in redox processes in soil [42]. In addition, GRs with a wide range of *x* have been synthetised and a variability of *x* ratio is found in fougerite, as exposed above. All these factors led to research on the redox potential of GRs, and especially on the natural capacity of fougerite to reduce pollutants in soils.

As for the crystallographic structure of fougerite, two models are proposed to explain its reductor potential. On one hand, a model based on a ternary solid solution of $Fe(OH)_2$, $Fe(OH)_3$ and $Mg(OH)_2$, and in the other hand a model based on the deprotonation reaction from GR1(CO_3^{2-}) to GR(CO_3^{2-})*.

6.2.1. Fougerite as a GR(OH^-): the ternary solid solution model

Fougerite is considered as a GR1(OH^-), with a similar structure to GR1(Cl^-), which is realistic since both anions have a spherical shape [2]. Since Mg^{2+} cations are incorporated at the structure, $Mg(OH)_2$ must be taken into account, assuming a ternary solution with end-members $Fe(OH)_2$, $Fe(OH)_3$ and $Mg(OH)_2$ [38].

This model implies that the main factor that causes the variability of *x* and thus, the reductant nature of fougerite is the partial substitution of Fe(II) by Mg(II). Arguing that such large variations in Mg^{2+} content in soil are not possible, among other arguments, this model is totally rejected by Génin et alt. [19], who proposed a model based on the carbonate-fougerite and its deprotonation reaction.

6.2.2. Fougerite as a GR(CO_3^{2-}): oxidation by the deprotonation reaction

The redox flexibility of fougerite can be explained if GR1(CO_3^{2-}) is supposed as the natural GR. It has been proved in laboratory conditions that GR1(CO_3^{2-}) has a redox flexibility from x = 0 to x = 1, and it can exist in a continuous domain between these two values. In order to explain this flexibility two counterparts of the stoichiometric GR must be described: a ferrous hydroxycarbonate GR1(CO_3^{2-})§ and a ferric oxyhydroxycarbonate GR1(CO_3^{2-})*.

The stoichiometric GR1(CO_3^{2-}) is the one described in section 6.1.4.2. The most paradigmatic compound is described when *x* = 1/3 (point a in Figure 4). In this case, every Fe cation is surrounded by 6 OH^-.

The ferrous hydroxycarbonate GR1(CO_3^{2-})§ is the compound obtained when GR1(CO_3^{2-}) is protonated. In the extreme case, when *x* = 0 (point b in Figure 4), all Fe(II) cations in GR1(CO_3^{2-}) are reduced to Fe(II), and every Fe(II) cation is surrounded by 5 OH^- and one H_2O molecule [4].

In contrast, the ferric oxyhydroxycarbonate GR1(CO_3^{2-})* is obtained when GR1(CO_3^{2-}) is deprotonated. Again, for the extreme case, when *x* = 1 (point c in Figure 4) all Fe cations are oxidised to Fe(III), and every Fe(III) cation is surrounded by 4 OH^- and 2 O^{2-} [19].

These three cases are the most exemplifying, but the redox flexibility of the GR1(CO_3^{2-}) must be understood as a continuous domain, and the transformations (protonation or deprotonation and Fe^{n+} oxidation or reduction) as a progressive transformation, represented by the gradient vector in Figure 4. This half redox reaction can be generalised as following [4]:

$$Fe_4^{2+}Fe_2^{3+}(OH)_{12}CO_3 + 2(1-3x)H^+ + 2(1-3x)e^- \rightarrow Fe_{6(1-x)}^{2+}Fe_{6x}^{3+}O_{12}H_{2(7-3x)}CO_3 \quad (1)$$

describing an oxidation when x > 1/3 and a reduction when x < 1/3. Must be underlined that in any moment along the reaction, the crystalline structure is changed, only a shrinkage of the distance between cations is observed when GR1(CO_3^{2-}) is oxidated into GR1(CO_3^{2-})*, XRD, TMS and SEM analyses have been done to confirm it [19].

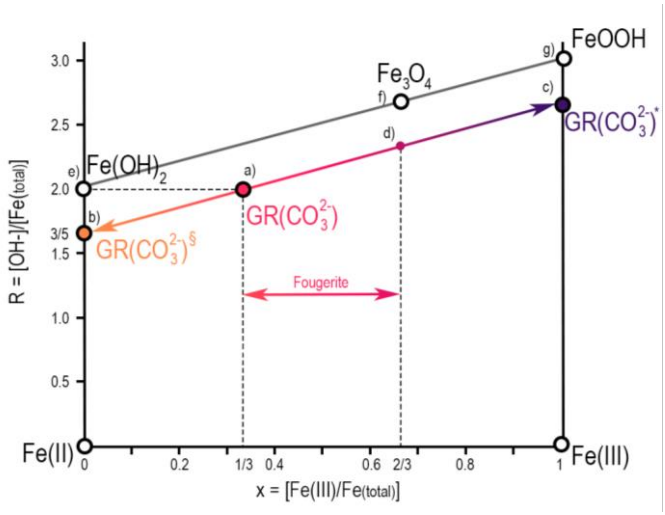

Figure 4. Mass diagram drawn in order to describe graphically the redox process. The diagram is built by plotting R = $[OH^-]/[Fe_{total}]$ versus x = $[Fe(III)/Fe_{total}]$. Adapted from [4].

As said before, that redox flexibility is proved from x = 0 to x = 1 at the laboratory, but what about the fougerite in natural conditions? Analyses of field samples shown a range of values from x = 1/3 to x = 2/3 (see section 6.1.5.3), which is enough redox flexibility to reduce some pollutants in soil. It is demonstrated that in field conditions GR1(CO_3^{2-}) with x = 0.33 (point a in Figure 4) can oxidise following the deprotonation reaction (1) until it reaches an x = 0.67 value (point d in Figure 4), and then, GR1(CO_3^{2-})* continues its oxidation but turning into magnetite (point f in Figure 4) and subsequently to ferric oxyhydroxides (such as ferroxyhite, δ' FeOOH, point g in Figure 4) [13]. Thus, the mineral fougerite is described as the compound comprised on the interval 1/3 < x < 2/3.

In detail, fougerite is mostly produced in nature by the action of Dissimilatory Iron-Reducing Bacteria (DIRB), that substitute oxygen for Fe(III) (taken from the ferric oxyhydroxides FeOOH)

to supply their need of an electron acceptor for the respiration, and consequently Fe(II) cations are released [19]. The same bacteria respiration process releases CO_2 that is actually present as HCO_3^- ions in solution, so all the components to form GR1(CO_3^{2-}) are produced at the same time and place, and the following reaction takes place:

$$6xFe^{3+}OOH + 6(1-x)Fe^{2+} + HCO_3^- + 12(1-x)H_2O \rightarrow$$
$$Fe_6O_{12}H_{2(7-3x)} + (11-12x)H^+ \quad (2)$$

Then, the fougerite formed can react with the pollutant to reduce it and get oxidised again to form FeOOH, creating a cycle [39].

Therefore, two reasons are extracted to justify that fougerite is one of the most important natural agents in the reduction of pollutants in hydromorphic soils:

- Redox potential of fougerite is adjusted without changing the crystallographic structure.
- Fougerite is regenerated by natural bacteria activity in a cyclic way.

In addition, if fougerite is compared with other similar minerals (like pyroaurite or hydrotalcite) the first one has a higher reductor power because the divalent and the trivalent cation are from the same element, iron, so no diffusion of different elements is necessary to oxidate the compound, which makes easier the process [19].

6.2.3. Reduction of pollutants by GRs

It has been demonstrated that many pollutants can be reduced by GRs, both synthetic ones and fougerite. First, the NO_3^- case will be exposed, and afterwards, a review of other chemical species reduced by GR will be done.

6.2.3.1. Nitrate reduction by fougerite

For the case of nitrogen, for which many studies have been carried out, the cycle of fougerite could be summarised as shown in Figure 5. The nitrate case is of special interest due to the importance that the soil pollution by nitrates has in zones where the agricultural activity is important and the consequences that it can have [11].

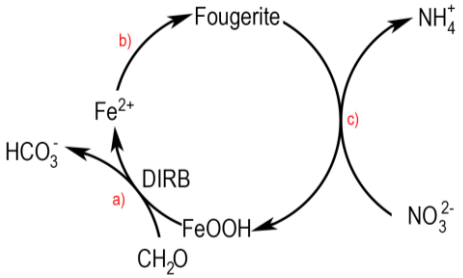

Figure 5. Cycle of nitrate reduction by fougerite. Reaction (a): reduction of Fe(III) by the DIRB action in anoxic conditions, where CH_2O is the organic matter that bacteria need as a source of energy, and Fe(II) and HCO_3^- ions are produced. Reaction (b): the ions produced are used to form fougerite, following reaction (2). Reaction (c): fougerite reduces NO_3^- into NH_4^+, that oxidises easily to N_2 that leaks without harming the environment [13], [19], [39].

6.2.3.2. Other chemical species reduced by GRs

In Table 10 are summarised different metal ions and compounds that are reduced by GRs found in literature and a brief description of the reduction conditions. The reduction of these chemical species has special relevance either because most of them are considered as pollutants, or because by reducing them, its mobility changes and it has an impact in their geochemical cycles.

Pollutant	*Conditions*	*Reference*
Cr^{6+}	Cr^{6+} is reduced to Cr^{3+} by a synthetic GR1(CO_3^{2-}) in hydromorphic soils pH conditions. Reaction is limited if GR is not regenerated.	[14]
	Cr^{6+} is reduced to Cr^{3+} by a synthetic GR2(SO_4^{2-}) following a different mechanism: CrO_4^{2-} substitutes SO_4^{2-} and gets reduced.	[43]

Hg^{2+}, Cu^{2+}, Au^{3+}, Ag^{+}	Hg^{2+}, Cu^{2+}, Au^{3+}, Ag^{+} are reduced to Hg^{0}, Cu^{0}, Au^{0}, Ag^{0} by a synthetic GR2(SO_4^{2-}).	[44]
Se^{6+}	Se^{6+} is reduced to Se^{4+} and Se^{0} by a synthetic GR2(SO_4^{2-}).	[45]
U^{6+}	U^{6+} is reduced to U^{4+} by a synthetic GR2(SO_4^{2-}) and UO_2 nanoparticles are formed.	[46]
CCl_4	Reductive dechlorination by a synthetic GR2(SO_4^{2-}) that leads to $CHCl_3$ and C_2Cl_6.	[23]
cis-DCE, VC	Reductive dechlorination by a mixed chloride/sulphate GR that leads to ethene and ethane.	[47]
PCE, TCE, cis-DCE, VC	Reductive dichlorination by a synthetic GR2(SO_4^{2-}) that leads to acetylene, ethene and ethane.	[15]

Table 10. Summary of different chemical species reduced by GR found in literature. Abbreviations: Tetrachloroethene (PCE), Trichloroethene (TCE), cis-Dichloroethene (cis-DCE), Vinyl Chloride (VC).

6.3. ABIOTIC REDUCTION OF CHLORINATED ETHENES

During some years, the study of the dechlorination of chlorinated ethenes and the possibility to remediate natural aquifers polluted with these compounds has focused on the biotic reactions that can reduce them, forgetting about the abiotic ways that also reduce them [12]. In particular, GR is one of the mixed Fe(II)-Fe(III) compounds that can reduce chlorinated ethenes due to their redox potential explained in section 6.2. and the precedent studies where GR was demonstrated to reduce chlorinated alkanes [23], [48].

The pollution with this kind of compounds, which mostly came from the metal industry, dry cleaning or extraction processes, is of special interest due to their persistence in natural environments and toxicity [49].

Thus, a review on the abiotic reduction of chlorinated ethenes but also on the interdependence between biotic and abiotic processes will be done.

6.3.1. Pathways and products

Abiotic dechlorination of organic chlorinated compounds can go through reductive elimination, hydrogenolysis, dehydrohalogenation or hydrolysis. For chlorinated alkenes, the most important mechanisms are reductive eliminations but also hydrogenolysis (in a minor grade). A summary of the possible reaction pathways and products of the chlorinated ethenes is shown in Figure 6. When the reduction of PCE is studied, it is found that PCE is principally reduced to acetylene, which is used as a sign that an abiotic dechlorination process is taking place. Acetylene can reduce even more to ethene and ethane. These observations are done for several minerals such as FeS, magnetite or GR [12], [15], [50], [51]. It is also observed that as much chlorinated is the compound, more susceptible is it to go through a dechlorination [52].

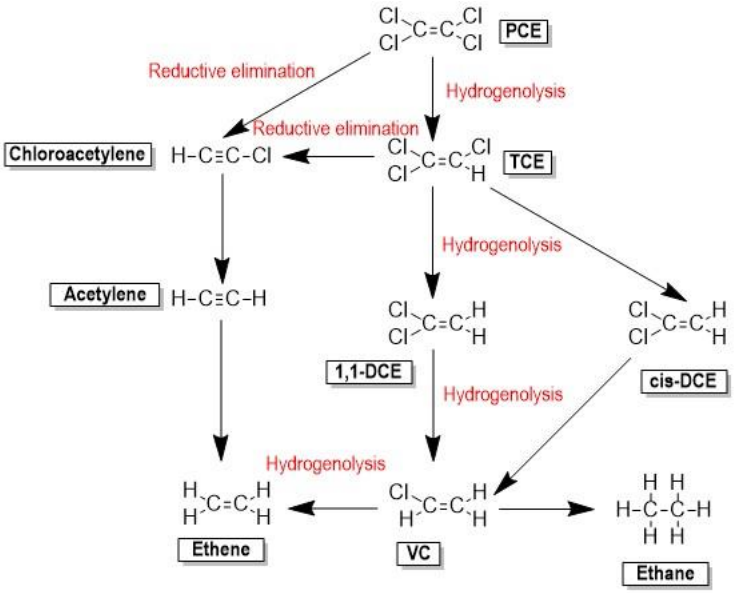

Figure 6. Pathways and products of abiotic reduction of chlorinated ethenes [12].

These abiotic reactions are found to be surface mediated, which implies that a bigger surface will lead to a faster reduction [12], [23].

6.3.2. Different Fe(II) containing minerals that can reduce chlorinated ethenes

Different Fe(II) containing minerals show different reactivities while reducing chlorinated compounds. A review work done by He et al. [12] established that the trend of mineral reactivity for this kind of reactions is: disordered FeS > FeS > Fe(0) > FeS_2 > sorbed Fe(II) > GR = magnetite > biotite = vermiculite.

In particular for the GR case, it has been observed that the kinetics of the dechlorination reaction starts with a rapid disappearance of the initial chlorinated ethene, but the reaction slows down due to the oxidation of GR to magnetite (Fe_3O_4) or maghemite (γ-Fe_2O_3). PCE reduction leads mainly to acetylene [15]. This is the main limitation of biotic reduction reactions.

6.3.3. Interdependence between biotic and abiotic processes

Even it is out of the main scope of this work, biotic (or microbial) processes must be considered if the dechlorination of chlorinated ethenes is pretended to be described. Microbial dechlorination usually involves mechanisms like halorespiration (a type of anaerobic respiration) [53] or co-metabolism i.e. when bacteria use their enzymes that initially were used to other porpoises to reduce these compounds in presence of another organic substrate that acts as an energy source [49], [54]. The main weakness of a biotic isolated process is that can lead to an incomplete dechlorination of the mother compounds (PCE and TCE) and produce chlorinated daughter compounds such as both isomers of DCE or VC, which are even more toxic than the original ones [15], [52], [55].

Therefore, it is important to focus on the interactions between biotic and abiotic processes, not only because of the limited partial dechlorination carried on by the microorganisms but also because of the potential that these interactions have to improve remediations processes. This complementarity of biotic and abiotic processes that can lead to a satisfactory dechlorination of chlorinated ethenes can be described as:

- Biotic processes enhance the abiotic ones: the presence of microorganisms and its activity can lead to the formation of reactive materials that can reduce abiotically chlorinated ethenes. The case of fougerite explained in section 6.2.2. is a good example, but also other processes that involve biogenic minerals such as FeS, have been described [56]. This biological regeneration of minerals can solve the main limitation of abiotic processes, the depletion of these minerals.

- Abiotic processes enhance the biotic ones: the main product of abiotic reduction of PCE and TCE is acetylene, that can be degraded to ethene or ethanol by microorganisms or can serve as an electron donor for the halorespiration of microorganisms [49].

Evidence of this synergistic interaction between both type of processes is observed when the same experiment of reduction of chlorinated ethenes by magnetite is done with and without adding Fe(II), and when it is added, more reactivity is observed. It shows that Fe(II) (in this experiment added artificially but in natural systems released by bacteria) can regenerate reductive minerals (in that case, magnetite) and enhance the dechlorination [50].

7. CONCLUSIONS

A review on the published bibliography about GR has been done, and the topics considered as an objective have been analysed.

The main techniques used in the characterisation of GR are TMS and XRD. Other techniques are also used, such as TEM or SEM. Since GR are compounds that easily oxidise, careful procedures must be followed when samples are treated and prepared for every technique analyses. These general procedures are described but many studies seem to assume them and they do not elaborate on this topic.

Crystallographic structure of GR can be summarised as a stacking sequence of $Fe(OH)_2$ layers with some Fe(III) cations substituting that provides a positive charge, and interlayers composed of anions and water molecules. Two groups of GR have been described, GR1 and GR2. GR1 are formed by planar anions in the interlayer and the most common examples are GR1(Cl^-) and GR1(CO_3^{2-}). GR2 are formed by three-dimensional anions in the interlayer and the typical one is GR2(SO_4^{2-}). The specific structure of these three examples is described since is representative of all other GRs. Fougerite is described as the natural GR, being characteristic the partial substitution of Fe(II) by Mg(II) and the variability of its ratio $x = [Fe(III)/Fe_{total}]$. The anion in its interlayer depends on the soil conditions.

GRs are exceptional reductors since they have a wide redox flexibility due to their reactions of protonation and deprotonation, that gives a continuous domain of existence from $x = 0$ to $x = 1$ for synthetic GRs and a domain from $x = 0.33$ to $x = 0.67$ for fougerite. Fougerite is thought to be one of the most important minerals that reduces pollutants in hydromorphic soils.

In what concerns the reduction of chlorinated ethenes in polluted aquifers, its reduction it is not only due to the reductive action of GR. In fact, there coexist two processes, the biotic and the abiotic one (that includes the reduction by GR and by other Fe(II) minerals), very interconnected with each other. This work has been focused on the abiotic process, specifically in the role of GR, but in order to understand remediation processes in aquifers polluted by chlorinated ethenes, a

wide scope must be taken, including biotic and abiotic processes and the enhancement that occurs between them.

GRs are expected to be a key element on the remediation of different pollutants in soil, and they could be applied on a wide variety of future applications.

11. REFERENCES AND NOTES

[1] J. D. Bernal, D. R. Dasgupta, and A. L. Mackay, “The oxides and hydroxides of iron and their structural interrelations,” *Clay Miner. Bull.*, vol. 4, pp. 15–30, 1959.

[2] M. . T. Génin, J-M. R.; Refait, P.; Bourrié, G.; Abdelmoula, “Structure and stability of the Fe(II) - Fe(III) green rust....pdf,” *Appl. Geochemistry*, vol. 16, pp. 559–570, 2001.

[3] J. M. R. Génin and C. Ruby, “Structure of some FeII-III hydroxysalt green rusts (carbonate, oxalate, methanoate) from Mössbauer spectroscopy,” *Hyperfine Interact.*, vol. 185, no. 1–3, pp. 191–196, 2008.

[4] J. M. R. Génin, C. Ruby, and C. Upadhyay, “Structure and thermodynamics of ferrous, stoichiometric and ferric oxyhydroxycarbonate green rusts; redox flexibility and fougerite mineral,” *Solid State Sci.*, vol. 8, pp. 1330–1343, 2006.

[5] F. Trolard, “Fougerite: From field experiment to the homologation of the mineral,” *Comptes Rendus - Geosci.*, vol. 338, no. 16, pp. 1158–1166, 2006.

[6] P. Duchaufour, *Pedology*. Springer, Dordrecht, 1982.

[7] F. N. Ponnamperuma, E. M. Tianco, and T. Loy, “Redox equilibria in flooded soils,” *Soil Sci.*, vol. 103, no. 6, pp. 374–382, 1967.

[8] P. Refait, J. B. Memet, C. Bon, R. Sabot, and J. M. R. Génin, “Formation of the Fe(II)–Fe(III) hydroxysulphate green rust during marine corrosion of steel,” *Corros. Sci.*, vol. 45, no. 4, pp. 833–845, 2003.

[9] C. Bender Koch and S. Mørup, “Identification of green rust in an ochre sludge,” *Clay Miner.*, vol. 26, no. 4, pp. 577–582, 1991.

[10] F. . G. Trolard and M. . et al énin, J.-M. R.; Abdelmoula, “Identification of a green rust mineral in a reductomorphic soil by Mössbauer and Raman spectroscopies,” *Geochim. Cosmochim. Acta*, vol. 61, pp. 1107–111, 1997.

[11] L. H. G. Chaves, “The role of green rust in the environment: a review,” *Rev. Bras. Eng. Agrícola e Ambient.*, vol. 9, no. 2, pp. 284–288, 2005.

[12] Y. T. He, J. T. Wilson, C. Su, and R. T. Wilkin, “Review of Abiotic Degradation of Chlorinated Solvents by Reactive Iron Minerals in Aquifers,” *Groundw. Monit. Remediat.*, vol. 35, no. 3, pp. 57–75, 2015.

[13] J. M. R. Génin, A. Renard, and C. Ruby, “Fougerite FeII∈-∈III oxyhydroxycarbonate in environmental chemistry and nitrate reduction,” *Hyperfine Interact.*, vol. 186, no. 1–3, pp. 31–37, 2008.

[14] A. G. B. Williams and M. M. Scherer, “Kinetics of Cr(VI) reduction by carbonate green rust,” *Environ. Sci. Technol.*, vol. 35, no. 17, pp. 3488–3494, 2001.

[15] W. Lee and B. Batchelor, “Abiotic reductive dechlorination of chlorinated ethylenes by iron-bearing soil minerals. 2. Green rust,” *Environ. Sci. Technol.*, vol. 36, no. 24, pp. 5348–5354, 2002.

[16] F. Trolard, J. M. R. Génin, M. Abdelmoula, G. Bourrié, B. Humbert, and A. Herbillon, “Identification of a green rust mineral in a reductomorphic soil by Mössbauer and

Raman spectroscopies," *Geochim. Cosmochim. Acta*, vol. 61, no. 5, pp. 1107–1111, 1997.

[17] H. C. B. Hansen, "Composition, stabilization, and light absorption of Fe(II)Fe(III) hydroxy-carbonate ('green rust')," *Clay Miner.*, vol. 24, no. 4, pp. 663–669, 1989.

[18] J.-M. R. Refait, PH.; Abdelmoula, M.; Génin, "Mechanisms of Formation and Structure of Green Rust One in Aqueous Corrosion of Iron in the," *Corros. Sci.*, vol. 40, pp. 1547–1560, 1998.

[19] J. M. R. Génin *et al.*, "Fougerite and Fe II-III hydroxycarbonate green rust; ordering, deprotonation and/or cation substitution; structure of hydrotalcite-like compounds and mythic ferrosic hydroxide Fe(OH)(2+x)," *Solid State Sci.*, vol. 7, pp. 545–572, 2005.

[20] L. Simon, M. François, P. Refait, G. Renaudin, M. Lelaurain, and J. M. R. Génin, "Structure of the fe(II-III) layered double hydroxysulphate green rust two from Rietveld analysis," *Solid State Sci.*, vol. 5, pp. 327–334, 2003.

[21] F. Trolard, G. Bourrié, M. Abdelmoula, P. Refait, and F. Feder, "Fougerite, a new mineral of the pyroaurite-iowaite group: Description and crystal structure," *Clays Clay Miner.*, vol. 55, no. 3, pp. 323–334, 2007.

[22] C. A. Johnson, "Observations and Assessment of Iron Oxide Nanoparticles in Metal-Polluted Mine Drainage within a Steep Redox Gradient, and a Comparison to Synthetic Analogs," *J. Chem. Inf. Model.*, vol. 53, no. 9, pp. 1689–1699, 2013.

[23] M. Erbs, H. C. B. Hansen, and C. E. Olsen, "Reductive dechlorination of carbon tetrachloride using iron(II) iron(III) hydroxide sulfate (green rust)," *Environ. Sci. Technol.*, vol. 33, no. 2, pp. 307–311, 1999.

[24] J. M. R. Génin and C. Ruby, "Anion and cation distributions in Fe (II-III) hydroxysalt green rust from XRD and Mössbauer analysis (carbonate, chloride, sulphate,...); the 'fougerite' mineral," *Solid State Sci.*, vol. 6, pp. 705–718, 2004.

[25] E. Murad and R. M. Taylor, "The Mössbauer spectra of hydroxycarbonate green rusts," *Clay Miner.*, vol. 19, no. 1, pp. 77–83, 1984.

[26] A. H. Cuttler, V. Man, and T. E. Cranshaw, "A Mössbauer study of Green Rust precipitates: I. Preparations from sulphate solutions," *Clay Miner.*, vol. 25, pp. 289–301, 1990.

[27] P. Refait, M. Abdelmoula, F. Trolard, J. M. R. Génin, and G. Bourkié, "Mössbauer and XAS study of a green rust mineral; The partial substitution of Fe2+ by Mg2+," *Am. Mineral.*, vol. 86, no. 5–6, pp. 731–739, 2001.

[28] C. A. Johnson, M. Murayama, K. Küsel, and M. F. Hochella, "Polycrystallinity of green rust minerals and their synthetic analogs: Implications for particle formation and reactivity in complex systems," *Am. Mineral.*, vol. 100, no. 10, pp. 2091–2105, 2015.

[29] A. Géhnin *et al.*, "Synthesis of Fe(II-III) hydroxysulphate green rust by coprecipitation," *Solid State Sci.*, vol. 4, pp. 61–66, 2002.

[30] I. Halevy, M. Alesker, E. M. Schuster, R. Popovitz-Biro, and Y. Feldman, "A key role for green rust in the Precambrian oceans and the genesis of iron formations," *Nat. Geosci.*, vol. 10, no. 2, pp. 135–139, 2017.

[31] M. Usman, K. Hanna, M. Abdelmoula, A. Zegeye, P. Faure, and C. Ruby, "Formation of green rust via mineralogical transformation of ferric oxides (ferrihydrite, goethite and hematite)," *Appl. Clay Sci.*, vol. 64, pp. 38–43, 2012.

[32] J. M. Bearcock, W. T. Perkins, E. Dinelli, and S. C. Wade, "Fe(II)/Fe(III) 'green rust'

developed within ochreous coal mine drainage sediment in South Wales, UK," *Mineral. Mag.*, vol. 70, no. 6, pp. 731–741, 2006.

[33] C. Su and R. W. Puls, "Significance of iron (II,III) hydroxycarbonate green rust in arsenic remediation using zerovalent iron in laboratory column tests," *Environ. Sci. Technol.*, vol. 38, no. 19, pp. 5224–5231, 2004, doi: 10.1021/es0495462.

[34] "Selected area diffraction - Wikipedia." https://en.wikipedia.org/wiki/Selected_area_diffraction (accessed Nov. 19, 2020).

[35] J. M. R. Génin, M. Abdelmoula, P. Refait, and L. Simon, "Comparison of the green rust two lamellar double hydroxide class with the green rust one pyroaurite class : Fe(II)-Fe(III) sulphate and selenate hydroxides," *Hyperfine Interact.*, vol. 3, pp. 313–316, 1998.

[36] R. Aïssa *et al.*, "formation and crystallographical structure of hydroxysulphate and hydroxycarbonate green rusts synthetised by coprecipitation," *J. Phys. Chem. Solids*, vol. 67, pp. 1016–1019, 2006.

[37] M. Abdelmoula, F. Trolard, G. Bourrié, and J. M. R. Génin, "Evidence for the Fe(II)-Fe(III) Green Rust 'Fougerite' mineral occurrence in a hydromorphic soil and its transformation with depth," *Hyperfine Interact.*, vol. 112, pp. 235–238, 1997.

[38] G. Bourrié, F. Trolard, P. Refait, and F. Feder, "A solid-solution model for Fe(II)-Fe(III)-Mg(II) green rusts and fougerite and estimation of their Gibbs free energies of formation," *Clays Clay Miner.*, vol. 52, no. 3, pp. 382–394, 2004.

[39] C. Ruby, C. Upadhyay, A. Géhin, G. Ona-Nguema, and J. M. R. Génin, "In situ redox flexibility of FeII-III oxyhydroxycarbonate green rust and fougerite," *Environ. Sci. Technol.*, vol. 40, no. 15, pp. 4696–4702, 2006.

[40] F. Trolard and G. Bourri, "Fougerite a Natural Layered Double Hydroxide in Gley Soil: Habitus, Structure, and Some Properties," *Clay Miner. Nat. - Their Charact. Modif. Appl.*, vol. 9, pp. 171–188, 2012.

[41] F. Feder, F. Trolard, G. Klingelhöfer, and G. Bourrié, "In situ Mössbauer spectroscopy: Evidence for green rust (fougerite) in a gleysol and its mineralogical transformations with time and depth," *Geochim. Cosmochim. Acta*, vol. 69, no. 18, pp. 4463–4483, 2005.

[42] K. A. Weber, L. A. Achenbach, and J. D. Coates, "Microorganisms pumping iron: Anaerobic microbial iron oxidation and reduction," *Nat. Rev. Microbiol.*, vol. 4, no. 10, pp. 752–764, 2006.

[43] L. L. Skovbjerg, S. L. S. Stipp, S. Utsunomiya, and R. C. Ewing, "The mechanisms of reduction of hexavalent chromium by green rust sodium sulphate: Formation of Cr-goethite," *Geochim. Cosmochim. Acta*, vol. 70, no. 14, pp. 3582–3592, 2006.

[44] O. E. J, S. D. Kelly, K. M. Kemner, R. Csencsits, and R. E. Cook, "Reduction of AgI, AuIII, CuII and HgII by FeII/FeIII hydroxysulfate green rust," *Chemosphere*, vol. 53, pp. 437–446, 2003.

[45] S. C. B. Myneni, T. K. Tokunaga, and G. E. Brown, "Abiotic selenium redox transformations in the presence of Fe(II,III) oxides," *Science (80-.).*, vol. 278, pp. 1106–1109, 1997.

[46] E. J. O'Loughlin, S. D. Kelly, R. E. Cook, R. Csencsits, and K. M. Kemner, "Reduction of uranium(VI) by mixed iron(II)/iron(III) hydroxide (green rust): Formation of UO2 nanoparticles," *Environ. Sci. Technol.*, vol. 37, no. 4, pp. 721–727, 2003.

[47] Y. S. Han, S. P. Hyun, H. Y. Jeong, and K. F. Hayes, “Kinetic Study of cis-dichloroethylene (cis-DCE) and vinyl chloride (VC) dechlorination using green rusts formed under varying conditions,” *Water Res.*, vol. 46, pp. 6339–6350, 2012.

[48] E. J. O’Loughlin and D. R. Burris, “Reduction of halogenated ethanes by green rust,” *Environ. Toxicol. Chem.*, vol. 23, no. 1, pp. 41–48, 2004.

[49] P. Bhatt, M. Suresh, S. Mudliar, and T. Chakrabarti, “Biodegradation of Chlorinated Compounds-A Review,” *Crit. Rev. Environ. Sci. Technol.*, vol. 37.

[50] W. Lee and B. Batchelor, “Abiotic reductive dechlorination of chlorinated ethylenes by iron-bearing soil minerals. 1. Pyrite and magnetite,” *Environ. Sci. Technol.*, vol. 36, no. 23, pp. 5147–5154, 2002.

[51] H. Y. Jeong, H. Kim, and K. F. Hayes, “Reductive dechlorination pathways of tetrachloroethylene and trichloroethylene and subsequent transformation of their dechlorination products by mackinawite (FeS) in the presence of metals,” *Environ. Sci. Technol.*, vol. 41, no. 22, pp. 7736–7743, 2007.

[52] T. M. Vogel, C. S. Criddle, P. L. McCarty, and J. C. Arcos, “Transformations of halogenated aliphatic compounds: Oxidation, reduction, substitution, and dehydrohalogenation reactions occur abiotically or in microbial and mammalian systems,” *Environ. Sci. Technol.*, vol. 21, no. 8, pp. 722–736, 1987.

[53] C. Holliger, G. Schraa, A. J. M. Stams, and A. J. B. Zehnder, “A highly purified enrichment culture couples the reductive dechlorination of tetrachloroethene to growth,” *Appl. Environ. Microbiol.*, vol. 59, no. 9, pp. 2991–2997, 1993.

[54] EPA, “Proceedings of the Symposium on Natural Attenuation of Chlorinated Organics in Groundwater,” in *Biotic and abiotic transformations of chlorinated solvents in ground water*, 1997, pp. 7–11.

[55] EPA, “Proceedings of the Symposium on Natural Attenuation of Chlorinated Organics in Groundwater,” in *Microbiological aspects relevant to natural attenuation of chlorinated ethenes*, 1997, pp. 12–15.

[56] E. C. Butler, L. Chen, and R. Darlington, “Transformation of trichloroethylene to predominantly non-regulated products under stimulated sulfate reducing conditions,” *Groundw. Monit. Remediat.*, vol. 33, no. 3, pp. 52–60, 2013.

12. ACRONYMS

Cis-DCE (cis-Dichloroethene)

DSC (Differential Scanning Calorimetry)

GR (Green Rust)

IMA (International Mineralogical Association)

LDH (Layered Double Hydroxyy)

PCE (Tetrachloroethene)

RA (Relative Abundance)

SEM (Scanning Electronic Microscopy)

TCE (Trichloroethene)

TEM (Transmission Electronic Microscopy)

TMS (Transmission Mössbauer Spectroscopy)

VC (Vinyl Chloride)

XAS (X-ray Absorption Spectroscopy)

XRD (X-Ray Diffraction)

APPENDICES

APPENDIX 1: GR1(Cl^-) ANALYSES RESULTS

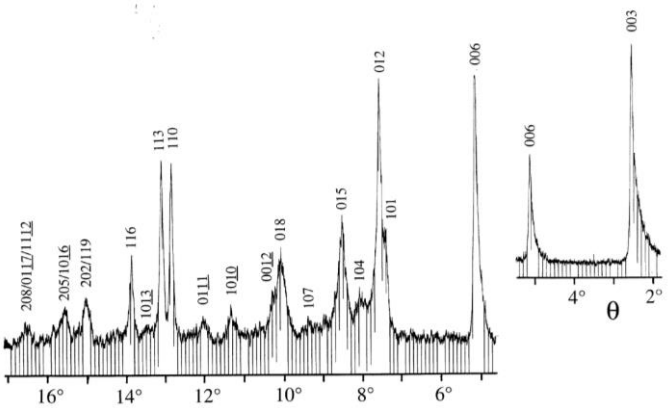

Figure 7. X-ray diffraction patern for GR1(Cl^-) [18].

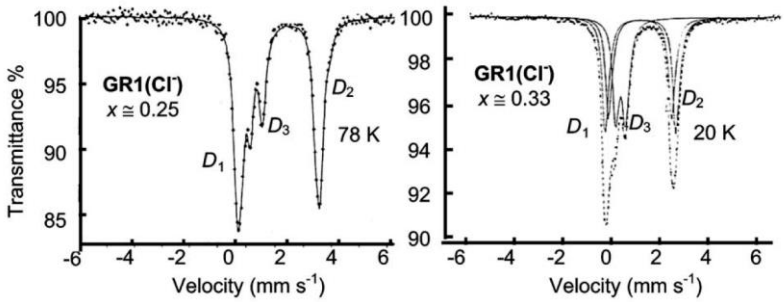

Figure 8. Mössbauer spectra for GR1(Cl^-) of different compositions [24].